Aircraft-based observation of volatile organic compounds (VOCs) over the North China Plain

Yibo Huangfu[1,#], Ziyang Liu[1,#], Bin Yuan[1,*], Sihang Wang[1], Xianjun He[1], Wei Zhou[2], Fei Wang[2], Ping Tian[2], Wei Xiao[2], Yuanmou Du[2], Jiujiang Sheng[2,*], Min Shao[1]

[1] College of Environment and Climate, Institute for Environmental and Climate Research, Guangdong-Hongkong-Macau Joint Laboratory of Collaborative Innovation for Environmental Quality, Jinan University, Guangzhou 511443, China

[2] Beijing Weather Modification Center, Beijing 100089, China

[#] These authors contributed equally to this work

[*] Corresponding author: Bin Yuan (byuan@jnu.edu.cn), Jiujiang Sheng (jiujiangsheng@163.com)

Abstracts.

The vertical distribution of reactive trace gases can greatly help understand the complex atmospheric evolution under the joint impacts of surface emission, chemical removal, and regional transport. Focusing on the core area of the North China Plain, aircraft-based observations were conducted in September 2017 and July 2019 to reveal the vertical distributions of volatile organic compounds (VOCs) measured by high-time resolution mass spectrometry. Generally decreasing trends of VOC concentrations with altitudes were captured, indicating strong surface source emissions and chemical removal within the planetary boundary layer (PBL). Ethanol exhibited the highest concentration within the PBL with an average of 46.7 ppbv and the largest ratio (16.5) between the average below and above the PBL heights. The vertical-averaged VOCs above Baoding were greater than those in Beijing by factors ranging from 1.2 to 3.5, suggesting richer precursors for secondary pollutant formation in Baoding. Increases of several VOC species, including styrene and acetonitrile, at high altitudes (>2500 m) were captured in Beijing. Correlation analysis further revealed the significant influences of industrial and biomass burning emissions. Our results highlight the critical role of both local emissions and regional transport in shaping the VOC vertical distributions, which may affect atmospheric organic chemistry across various atmospheric layers in the region.

Keywords: Vertical profiles; aircraft-based observation; volatile organic compounds

1 Introduction

The North China Plain (NCP) stands as one of the most developed city clusters in China, yet it is also a region of concern that suffers from severe air pollution (Zhao et al., 2021;Yao et al., 2022b;Le et al., 2020;Wang et al., 2023). Following the implementation of the Action Plan on the Prevention and Control of Air Pollution, the particulate matter concentrations in NCP have significantly declined primarily due to a sharp reduction in anthropogenic emissions. In contrast, ozone levels have not shown a similar downward trend (Chen et al., 2020;Li et al., 2019a;Lu et al., 2019;Lu et al., 2020). From 2013 to 2019, the annual maximum daily average of 8-h ozone ($MDA8O_3$) concentrations increased significantly with a rate of 2.3 ppbv yr^{-1} in Beijing (Chen et al., 2020), while during warm seasons (Apr. – Sep.), the average increasing rate reached 3.3 ppbv yr^{-1} for NCP (Lu et al., 2020). Under the background of coordinated efforts to reduce pollution and carbon emissions, the continuous improvement of ambient air quality in the NCP region is under great pressure.

Volatile organic compounds (VOCs), as the key precursors of ozone and secondary organic aerosols due to photochemical degradation, have been listed as one of the key indicators for atmospheric environmental quality during the "14th Five-Year Plan" period (Li et al., 2022b;Mao et al., 2021). The temporal variation, emission characteristics, and environmental effect of VOCs have been extensively studied in the NCP region through ground-based measurements, greatly enhancing the understanding of the role in the formation of photochemical pollution (Yuan et al., 2012;Wang et al., 2014;Li et al., 2019b;Zhao et al., 2021;Sun et al., 2018;Forster et al., 2023). However, recent studies have also revealed the complex evolution of VOCs in the atmosphere under the impact of meteorological conditions (Zhang et al., 2018;Shi et al., 2018) and inter-city and regional transport (Liu et al., 2019;Zhao et al., 2021;Chang et al., 2019) that cannot be thoroughly investigated based on ground measurements.

In the past few years, vertical observations have been carried out utilizing observation towers (Zhang et al., 2020;Li et al., 2022a;Yang et al., 2024a;Li et al., 2024), tethered balloons (Zhang et al., 2019;Sangiorgi et al., 2011;Zhang et al., 2018), unmanned aerial vehicles (UAVs) (Peng et al., 2015;Han et al., 2016;Vo et al., 2018), and aircraft (Benish et al., 2020;Forster et al., 2023;Zhao et al., 2021;Wilde et al., 2021), bringing the opportunity to study VOCs from a three-dimensional perspective. Compared to other vertical observation techniques, aircraft platforms offer distinct

Deleted: ,

Deleted: ,

Deleted: however

advantages, including the capability of covering larger spatial areas, carrying heavy instrument payloads, and performing both vertical and horizontal observations at higher altitudes (Kwak et al., 2020;Zhao et al., 2021;Dieu Hien et al., 2019). The advantages of aircraft measurement make it an irreplaceable role in scientific research and practical applications. While aircraft-based research has been conducted intensively in the United States and Europe with high temporal resolution instruments (Fisher et al., 2016;Karion et al., 2015;Ren et al., 2018), only a handful of similar aircraft flights have been conducted equipped with online instruments that measure inorganic pollutants and aerosols in China (Zhao et al., 2021;Liu et al., 2018). Limited aircraft-based VOC measurements in China typically applied the collection of canister samples followed by detection by gas chromatography techniques in the laboratory (Xue et al., 2011;Benish et al., 2020;Liu et al., 2013). A typical decrease of non-methane hydrocarbons with increasing height was reported over Northeast China (Xue et al., 2011), while for the NCP region, aircraft-based measurements have been conducted but only reported the vertical distributions of BTEX species (benzene, toluene, ethylbenzene, xylenes), showing a similar negative trend with height (Liu et al., 2013). Nevertheless, the vertical distribution of VOCs in the NCP region is still unclear due to the scarcity of offline samples, hindering the ability to accurately assess the impacts of local emissions and air mass transport on VOC levels.

Deleted: However

This study analyses aircraft-based observation results over the Beijing and Baoding area, the two core cities of the NCP region. A proton transfer reaction time-of-flight mass spectrometer (PTR-ToF-MS) was equipped on the platform to monitor VOC concentrations with high time resolution across altitudes. Combined with correlation analysis of VOC pairs, possible sources and origins of VOCs within the planetary boundary layer (PBL) and the atmosphere above it were discussed, pointing out the important roles of local urban emissions and regional transport.

2 Methods

2.1 Aircraft flight routes

A King Air 350ER aircraft (Hawker Beechcraft) was deployed and five flights were conducted between Sep. 9th and 15th in 2017, and an additional flight on July 14th, 2019. The flight trajectories are summarized in **Table 1** and illustrated in **Figure 1**. The aircraft was based at Shahe Airport (40°8'24" N, 116°19'48" E) in Changping District, Beijing, surrounded by villages, factories, and educational institutions. Four of the

flights in 2017 (Sep. 9th, 12th, 13th, and 15th) focused on the Beijing area, while the remaining two flights (Sep. 14th, 2017, and Jul. 14th, 2019) followed southwest trajectories over the forest area before turning southeast to the Baoding area and returning to Shahe Airport. During each flight, the aircraft maintained level flight at a given altitude before ascending or descending to the next predetermined flight level. The step intervals between altitudes were consistently maintained within approximately 150 to 200 meters.

2.2 VOC sample and meteorological data collection

A PTR-ToF-MS (PTR-ToF-MS-8000, Ionicon Analytik GmbH, Austria) was applied onboard to measure VOC concentrations during each flight. The time-of-flight mass spectrometry has been proven to have the capability of measuring VOCs at high time resolution over broad mass spectra (Wu et al., 2020a;Yuan et al., 2017). Ambient air was drawn through a 1.5-m-long PTFE tube at a flow rate of 15 L/min using a pump. A sub-stream of this air was then subsampled by the PTR-ToF-MS at a flow rate of 100 mL/min through a PTFE membrane particle filter. With a voyage speed of ~250 km/h of the aircraft, VOC concentrations were measured every 5 s, resulting in a spatial resolution of ~70 m. The PTR-ToF-MS was operated with a drift pressure of 2.2 mbar, E/N 135 Td, and reactor temperature of 60 °C. The raw spectral data of PTR-ToF-MS were processed using the Ionicon Data Analyzer (IDA, V2.0.1.0), including mass calibration, peak detection, peak fitting, and etc. The sensitivities of PTR-ToF-MS for various VOC species were calibrated with commercial standard gas (Apel-Riemer, Environmental Inc., USA) before each field campaign. The sensitivity of monoterpenes was calibrated based on the a-pinene in the standard gas. Both methyl vinyl ketone (MVK) and methacrolein (MACR) were included in the standard gas, so the sensitivity of MVK&MACR was calculated based on their summed concentrations. A total of 15 VOC species are reported in this study and listed in **Table S1** as well as the limits of detection (LODs) and propagated uncertainties. Based on the multi-level tests in the laboratory, the impacts of humidity on VOC sensitivities were evaluated to be less than 10% for the reported VOC species, so no correction was conducted, and the induced uncertainty was propagated to the overall uncertainties. The interferences of fragmentations, such as the impact of higher-carbon aldehydes and cycloalkanes on isoprene signal (m/z 69, $C_5H_8H^+$) and the impact of ethylbenzene on benzene signal

Deleted: Ambient air was introduced into the sampling device and then subsampled by the PTR-ToF-MS using Polytetrafluoroethylene (PTFE) tubing

Deleted: The sensitivities of PTR-ToF-MS for various VOC species were calibrated with commercial standard gas (Apel-Riemer, Environmental Inc., USA).

Formatted: Font: Bold

Deleted: A total of 15 VOC species are reported in this study and listed in **Table S1**. Based on the multi-level tests in the laboratory, the impacts of humidity on VOC sensitivities were evaluated to be less than 10% for the reported VOC species, so no correction was conducted.

Formatted: Subscript

Formatted: Subscript

Formatted: Superscript

(m/z 79, $C_6H_6H^+$), were not corrected, so the concentrations of isoprene and benzene might be overestimated due to these interferences.

In addition, the aircraft platform also carried instruments that recorded the meteorological parameters (AIMMS-20, Aventech Research Inc.), including temperature, relative humidity, and pressure. The vertical profiles of meteorological factors are shown in **Figure S1**. A global positioning system (GPS) was equipped to record the aircraft's position. All instruments were thoroughly inspected and air-tightly checked before each flight to ensure the quality and reliability of data. To minimize the impact of aircraft exhaust emissions on VOC measurement, the data measured during the first 2 minutes after the engine started were excluded from the profile data.

2.3 Height of planetary boundary layer

In this study, the height of planetary boundary layer (HPBL) was determined by the air parcel method (Zhao et al., 2020;Zhao et al., 2019), which was considered to be more accurate and less deviated by human subjective judgment compared with the visual observation method and data simulation method (Zhang et al., 2019). The air parcel method determines the HPBL based on the vertical profile change of the potential temperature (T_θ) during the adiabatic process (Zhang et al., 2018). The vertical profiles of potential temperature for each flight can be found in **Figure S1**. T_θ first decreases with height to a minimum and then increases. The HPBL is determined as the height where T_θ returns to its surface value. The HPBL during each ascending and descending stage is listed in **Table S2**. A 10% uncertainty is determined based on previous studies (Zhao et al., 2019;Zhang et al., 2014;Vogelezang and Holtslag, 1996).

3 Results and discussion

3.1 The characteristics of VOC vertical distributions in Beijing

The ambient air quality data of criteria pollutants (ozone, NO_2, SO_2, CO, $PM_{2.5}$, and PM_{10}) of Changping Town station, the nearest national air quality monitoring station to the Shahe Airport (11 km away), were collected from the China National Environmental Monitoring Center (CNEMC) and presented in **Figure 2**. According to the Level-II thresholds in China's current National Ambient Air Quality Standards (NAAQS), pollution events in Beijing with $PM_{2.5}$ exceedances on Sep. 9th, 10th, and 14th and ozone exceedances on Sep. 13th were noticed. The vertical profiles of relative humidity (RH), temperature (T), and T_θ in **Figure S1** provide meteorological information for each flight. Monotonic trends for T and T_θ were recorded. T decreased

Formatted: Subscript
Formatted: Subscript
Formatted: Superscript
Formatted: Indent: First line: 2.5 ch
Deleted: when the air mass reaches the reference pressure (1000 hPa). The calculation formula of T_θ is: $T_\theta = T(\frac{1000}{P})^{\frac{R_d}{C_{pd}}}$ where P is the air pressure, T is the temperature under different air pressures, and R_d/C_{pd} is taken as 0.286 in this study
Formatted: Font: Bold
Formatted: Subscript
Deleted: The vertical profiles of meteorological factors are shown in **Figure S1**.
Formatted: Subscript
Deleted: NAQS

with altitude, while T_θ had opposite trends. In contrast, RH showed a more complex, non-monotonic trend with altitude, with great variations found across different aerial surveys, reflecting the complexity of the boundary layer structure.

Five flights were conducted over Beijing in Sep. 2017. The averaged concentrations of all 15 VOC species ranged from 25.9 ± 13.4 ppb measured on Sep.12th, 2017 to 52.1 ± 57.7 ppb measured on Sep.14th, 2017 (**Table S3**). The VOC concentrations measured within and above the PBL are listed in **Tables S4 and S5**. As illustrated in **Figure 3**, the VOC concentrations within the PBL (**Table S4**) were compared with previous measurements in urban Beijing (Squires et al., 2020;Yuan et al., 2012). Yuan et al. (2012) conducted VOC measurements on the top of a six-story building on Peking University campus using the PTR-MS technique in the summer of 2010. The concentrations of aromatic species below the PBL in this study were comparable to those measured in 2010 (**Figure 3b**), with data points clustering along the 1:1 line. For the OVOC species, the differences remained within or close to twofold variations. The two datasets in **Figure 3b** were measured seven years apart, during which VOC emissions in urban Beijing declined significantly(Wang et al., 2015;Yao et al., 2022a). While the VOC levels at the campus site in 2010 should have been higher due to greater VOC emissions, this effect was likely compensated for by the extra industrial emissions in suburban areas, which might be the reason for the comparable results observed.

VOC measurements by PTR-ToF-MS in the summer of 2017 were conducted at the 102 m platform of the Institute of Atmospheric Physics (IAP) meteorology tower and represented the VOC concentrations driven by traffic-related emissions in the center of urban Beijing (Squires et al., 2020). Compared with the 2017 IAP measurement, the aromatic species measured in this study were higher by factors ranging from 3.2 to 6.2 (**Figure 3c**). The enhancements of C8 and C9 aromatics are much greater than those of benzene and toluene. Given that industrial emissions contain higher proportions of C8 and C9 aromatics (Wang et al., 2024;Jiang et al., 2023), these results suggest that the VOC measured in aerial surveys in this study might be under the impacts of industrial emissions from the suburban region, especially at lower altitudes. Most OVOC species measured across both campaigns showed good agreement within twofold variability, except methyl ethyl ketone (MEK), which exhibited a factor of 5.7 higher in this study. As one of the common ingredients in industrial solvents, MEK can be emitted through multiple industrial processes (Wu et

Formatted: Superscript

Formatted: Superscript

Formatted: Font: Bold

Formatted: Font: Bold

Formatted: Font: Bold

Deleted: By contrast, compared with the 2017 measurement, the aromatic species measured in this study were higher by factors ranging from 3.2 to 6.2 (**Figure 3c**).

Deleted: Measurements in 2017 were made at the IAP meteorology tower represented the VOC concentrations driven by traffic-related emissions in the center of urban Beijing

Deleted: (Squires et al., 2020),

Deleted: while the VOC measured in aerial surveys in this study might be under the impact of industrial emissions from the suburban region, especially at lower altitudes

Deleted: As one of the common ingredients in industrial solvents, MEK can be emitted through multiple industrial processes

al., 2020b;Wang et al., 2024). Similarly, tetrahydrofuran (THF), an isomer of MEK and a significant industrial pollutant itself (Hu et al., 2018), may also contribute to the measured MEK signals. Hence, the higher concentrations of both compounds in this study are likely attributable to the nearby industrial emissions. Regarding the biogenic species, isoprene, MVK&MACR, and monoterpenes measured in this study were consistently higher than those reported in the other two campaigns, probably due to the enhanced biogenic emissions from the suburban region surrounded by mountain vegetation (**Figure 1**).

The characteristics of VOC vertical distributions were investigated through ten profiles obtained across the five flights over Beijing in 2017. Composite profiles of individual VOC species, as shown in **Figure 4**, revealed fundamental vertical distribution patterns, with detailed profiles for each flight provided in **Figures S2-S6**. Generally, decreasing trends with altitudes were observed for most VOC species, and the largest concentration variations were noticed towards the surface due to the dynamic change of surface emissions. These general decreasing trends of pollutants have been reported by previous studies (Benish et al., 2020;Liu et al., 2013;Xue et al., 2011). However, due to a lack of high-resolution VOC measurements, concentration variations with height and anomalous enhancement have not been documented.

All aromatic hydrocarbons exhibited characteristic negative vertical gradients with maximum concentrations at ground level (0.3-4.5 ppbv by average) and progressive decreases through the PBL, except the anomalous profile of styrene (**Figure 4**). Aromatic hydrocarbons primarily originate from vehicular and industrial emissions. and their lifetime within the PBL can span several days. The dominance of surface emissions explains their significantly higher concentrations near the ground than those measured above the the PBL. As turbulent mixing transports air upward, these compounds get oxidized with OH radicals, diminishing to near-zero levels at higher altitudes with minimal variation. The ground levels of C8 aromatics were the highest, reaching 4.5 ppbv on average. In contrast to other aromatic hydrocarbons, styrene displayed a distinct increase with altitude above the PBL, peaking notably at ~3500 m. Similar concentration enhancements at the same altitude were also observed for methanol, acetonitrile, and acetaldehyde. By checking the profiles of each flight (**Figures S2-S6**), such enhancements in the composite profiles were mainly driven by the measurement on Sep. 9th, 2017. This anomalous profile, potentially associated with long-range transported industrial emissions, will be further explored in **Section 3.3**.

Deleted: and higher concentrations in this study are likely attributable to the nearby industrial emissions

Deleted: methyl vinyl ketone and methacrolein (

Deleted:)

Deleted:

Formatted: Font: Bold

Formatted: Superscript

Formatted: Font: Bold

Similar VOC concentration enhancements were also found on the flight for Jul. 14th, 2019, which will be analyzed as well in **Section 3.3**.

OVOCs originate from both biogenic and anthropogenic sources and can also be formed as secondary products during the oxidation of non-methane hydrocarbons, complicating the interpretation of their vertical distributions (Yuan et al., 2012). Near the surface, OVOC concentrations were substantially higher than those of aromatic hydrocarbons. Across all flights, the vertical profiles of both alcohols and MEK followed trends similar to aromatic hydrocarbons. Their vertical variations demonstrate the impact of PBL dynamics, as evidenced by their pronounced vertical gradients (**Figure 4**). During the flight on Sep. 12th, the HPBL over Beijing exhibited the largest disparity between ascending and descending stages, with a difference of 700 m (**Table S2**). As illustrated in **Figure S3**, when the HPBL increased from ~900 m to ~1600 m, turbulent mixing transported ground methanol and ethanol upward, leading to a significant increase in alcohol concentrations above 1000 m. In contrast to other OVOCs, acetone and acetaldehyde displayed markedly greater variability above the PBL on Sep. 12th. Both compounds are known to form secondarily through atmospheric oxidation (Holzinger et al., 2005;de Gouw et al., 2004;Wu et al., 2020a), which likely contributes to their less uniform vertical distribution and larger variability at higher altitudes.

For biogenic VOCs, isoprene and monoterpenes are both primarily emitted from biogenic sources, while MVK and MACR are secondary oxidation products of isoprene (Canaval et al., 2020;Cappellin et al., 2019). Across all flight measurements, the vertical distribution patterns of MVK and MACR were quite similar to those observed for alcohols and most aromatic hydrocarbons. In contrast, the vertical profiles of isoprene and monoterpenes varied significantly between flights. Decreasing trends with altitude were found on Sep. 9th (**Figure S2**), Sep. 13th (**Figure S4**), and Sep. 14th (**Figure S5**). On Sep. 12th (**Figure S3**), there were no significant vertical variations of isoprene and monoterpenes across the altitudes. Notably, during the flight on Sep. 15th **(Figure S6)**, concentration enhancements can be seen at altitudes above 2000 m, suggesting a potential contribution from atmospheric transport.

The ratio between VOC species is commonly applied to address the impact of chemical removal and secondary formation during transport(Yang et al., 2024b;Zhu et al., 2025). The vertical profile of the C8 aromatics-to-acetone concentration ratio was plotted in **Figure 4** to demonstrate these effects. Both species can be emitted by

Formatted: Superscript

Deleted: This anomalous profile, potentially associated with upper-air biomass burning plumes or long-range transported industrial emissions, will be further explored in **Section 3.3**.

Formatted: Font: Bold

Formatted: Font: Bold

vehicular and industrial emissions (Jiang et al., 2023;Wang et al., 2024)), but C8 aromatics are more reactive, and acetone can be formed from secondary processes. The two effects both lead to a rapid decrease in the concentration ratio of C8 aromatics to acetone within the PBL before stabilizing as expected.

The averaged VOC concentrations measured below and above the PBL are compared in the scatter plot shown in **Figure 5**. To account for the variation of HPBL, data points above and below the light red area in **Figure 4** were used to calculate the averages and corresponding standard deviations. The averaged VOC concentrations below the PBL were consistently higher than those above the PBL, reflecting the combined effects of strong surface source emissions and the chemical oxidation process during vertical transport. Ethanol exhibited the highest concentration within the PBL with an average of 46.7 ppbv and the largest ratio of 16.5 between below- and above-PBL measurements. For the species with secondary formation, the data points of acetaldehyde, acetone, and MEK lay within the 2-5 ratio range. Above the PBL, the averaged concentrations of aromatic hydrocarbons were all smaller than 0.5 ppbv. Within the PBL, C8 aromatics showed the highest concentration, greater than the average above the PBL by a factor of 8.6, followed by toluene and benzene with factors of 6.6 and 5.4, respectively. C8 aromatics are quite chemically reactive, so a higher ratio suggests strong chemical removal, while for less reactive species, such as acetone, its ratio is closer to 1, indicating a weak impact of chemical reactions and potential contribution of secondary formation. Notably, the data points of styrene are clustered near the 1:1 ratio line, and occasionally, the concentrations above the PBL could be higher than those within the PBL. Since styrene is a primary species emitted at the surface, this pattern suggests a great contribution from transport, which will be discussed in **Section 3.3**. For isoprene, MVK and MACR, C9 aromatics, C10 aromatics, and acetonitrile, the average concentrations below the PBL were approximately twice as high as those measured above the PBL.

Deleted: To account for the variation of HPBL, data points above and below the grey area in

Deleted: were

Deleted: used to calculate the averages and corresponding standard deviations

Deleted: ,

Deleted: among which

Deleted: within the PBL

Deleted: and monoterpenes

Deleted: the ones

Deleted: Both species are primarily emitted at the surface, so this pattern suggests the transport influence

Formatted: Font: Bold

3.2 Differences in VOC vertical distribution in Beijing and Baoding

Two out of the six aerial surveys covered both the Beijing and Baoding areas. The aerial survey on Sep.14th, 2017 maintained a constant altitude of ~3000 m over Baoding, which prevented the collection of a vertical profile for Baoding. The flight conducted on Jul. 14th, 2019 provided comprehensive vertical distribution data for both cities through systematic altitude variations and therefore, was selected for the

comparative analysis of urban VOC profiles. As shown in **Figure S7**, the ascending stage over Beijing was quite short (<10 mins), so the vertical profiles measured during the descending stage at noon were selected to better represent the profiles in Beijing. The spiral descending stage in Baoding was used in the comparative analysis as it had well-designed altitude gradients.

The results of the comparison between the vertical VOC distributions of VOCs in Beijing and Baoding are illustrated in **Figure 6**. The VOC profile over Beijing exhibited notable concentration peaks around ~2500 m altitude, a feature previously observed during the flight on Sep. 9th, 2017 (**Figure S2)**. This anomaly will be discussed in **Section 3.3** through the ratio analysis. For Baoding, almost all the VOCs showed increasing trends with altitude, except for MVK and MACR, benzene, and toluene, with stable low levels above 1000 m altitude throughout the observation periods. Unfortunately, the aerial survey didn't capture the VOC surface measurements below 500 m in Baoding, which prevented the comparison between the near-ground VOC levels in both cities. Based on the ground monitoring data from local air quality monitoring stations (**Figure S8**), pollution episodes with ozone exceeding the Level-II NAAQS in both Beijing and Baoding were captured on Jul. 14th, 2019. Baoding exhibited much higher ozone concentrations compared to Beijing, indicating more severe photochemical pollution, and the northeast wind prevailing over Baoding suggests potential influence from regional transport from Beijing, as reported in previous studies (Huang et al., 2018). **Figure 7** presents the comparison between the averaged vertical concentrations of VOCs in Beijing and Baoding during the same altitude range (500-3000 m). Ethanol was found with the highest levels of VOCs measured in the air above both cities (**Figure 7a**), 98 ppbv for Beijing and 153 ppbv for Baoding, respectively. According to the scatter plot in **Figure 7b**, all the data points cluster around the 1:2 line. The VOC concentrations in Baoding were higher than those in Beijing by factors ranging from 1.2 to 3.5 with MEK showing the largest difference. Much greater concentrations of C8 and C9 aromatics in Baoding were found than those of benzene, which, together with the MEK showing the largest difference, suggests more significant impacts from the industrial emissions on the air above Baoding. This VOC enhancement implies a greater precursor reservoir over Baoding, which may accelerate secondary pollutant formation through chemical oxidation production and lead to more severe air pollution.

Deleted: NAQS

Deleted: 1.2 to 3.5 with MEK showing the largest difference, demonstrating consistent VOC enhancement patterns.

3.3 The contribution of regional emissions to VOC vertical profiles

Among six aerial surveys in 2017 and 2019, two distinct vertical distributions were noticed, characterized by abrupt VOC concentration enhancements above the PBL. For the aerial survey on Sep. 9th, 2017, the vertical profile of styrene exhibited an inverse gradient, with concentrations increasing from 0.2-0.3 ppbv at ground to peak levels of 0.6-1.0 ppbv at ~3500 m altitude, as shown in **Figure 8a**. Above the ~3500 m altitude, styrene concentration rapidly fell back to levels close to the detection limit by 4000 m. Similar increases at 3500 m were also noticed for methanol, acetonitrile, acetaldehyde, acetone, benzene, and C9 aromatics. By plotting the ratios of averaged VOC levels at altitudes of 2500-3500 m to the ones near the ground (0-500 m) in **Figure 8b**, only styrene showed a ratio significantly larger than 1. This anomaly indicates that at altitudes of 2500-3500 m, the VOC levels were influenced by air mass rich in styrene transported from further regions.

We further conducted a correlation analysis with styrene and benzene, as they can be co-emitted from common anthropogenic sources. The paired data points of styrene and benzene are shown in **Figure 8d,** together with ratio ranges representing industrial emissions (Jiang et al., 2023;Zhong et al., 2017), vehicular emissions (Wang et al., 2022), and ratios measured in urban Beijing at the IAP tower (He et al., 2025). The data points were color-coded with altitude. An obvious transition between two subsets of data can be seen as the altitude increases. The data points near the ground are all lying between the lines representing the characteristic ratios of diesel vehicles (slope = 0.32) and gasoline vehicles (slope = 0.08) and are consistent with the ratio observed at the Beijing IAP tower. This indicates the dominant contribution from vehicular emissions for the VOCs near the ground. In contrast, the data points observed with altitudes between 2500-3500 m are located in the characteristic ratio ranges related to industrial emissions, which suggests that the VOCs within this altitude range were greatly impacted by industrial emissions. The synoptic chart in **Figure S9a** shows strong northerly winds at the 850 hPa level over the aircraft survey area, suggesting that the industrial emissions were likely transported from the north. Since styrene is more chemically reactive than benzene and thus the lifetime of styrene is much shorter than that of benzene. The ratio of styrene to benzene would decrease during transport. As shown in **Figure 8d**, the enhancement ratios at higher altitudes still fall within the

Formatted: Font: Bold

Formatted: Font: Bold

characteristic ranges of industrial sources and are significantly larger than those of vehicular emissions. Thus, the chemical influences do not change our conclusion here.

During the aerial survey on Jul. 14th, 2019, the VOC vertical profiles in the Beijing area (**Figure 6**) showed similar trends with elevated VOC concentrations above 2500 m for almost all the VOCs. Analyses were conducted for this aerial survey as shown in **Figure 9**. The vertical levels of acetonitrile (**Figure 9a**), a widely applied tracer for biomass burning, were well above the typical backgrounds of 0.1-0.3 ppbv reported in previous studies (Wu et al., 2016;Wang et al., 2007). The ratios of averaged VOC levels at higher altitudes (2500-3000 m) and lower altitudes (<500 m) were plotted in **Figure 9b**. Unlike the ratios illustrated in **Figure 8**, most VOC species in the aerial survey on Jul. 14th had ratios around 1 or even greater than 2 for MEK, C10 aromatics, C9 aromatics, and styrene, showing the impact of significant regional transport. Elevated acetonitrile concentrations above the background might suggest biomass burning contribution. However, using acetonitrile as the biomass burning tracer in urban regions can be problematic (Huangfu et al., 2021;Coggon et al., 2016). Other sources (e.g., vehicular emissions) also emit acetonitrile, potentially interfering with the identification of dominant emission sources (Inomata et al., 2013;Valach et al., 2014). Further correlation analysis was conducted between acetonitrile and benzene in **Figure 9d**. Both are typical pollutants emitted from biomass burning and vehicular emissions, therefore, the specific emission ratio of acetonitrile and benzene for both sources can be used as references in the source analysis. We applied the ratio measured in central Beijing to represent the typical ratio of vehicular emissions. While only a few data points are near the typical ratio of urban vehicular emissions (slope = 0.75), most of the data points lie within the typical biomass burning ratio range, suggesting the influence of biomass burning emissions. No clear height-dependent classification can be found, which is distinguished from the analysis in **Figure 8d**. As shown in **Figure S9b**, winds were quite weak at 850 hPa in the aircraft survey area, suggesting that the elevated VOC concentrations were likely attributed to localized biomass burning emissions.

The analysis of two distinct vertical distributions reveals that regional transport of emissions, such as industrial and biomass burning, can significantly influence the VOC vertical profiles, and the associated chemical processes and environmental impact deserve further investigation.

Deleted: Most of the data points lie within the typical biomass burning ratio range and well above the typical ratio of urban vehicular emissions (slope = 0.74)

Formatted: Font: Bold

Formatted: Font: Bold

4 Conclusion

Aircraft-based observations were conducted to investigate the vertical distribution of VOCs over Beijing and Baoding, two core cities in the NCP region. According to the vertical profiles of VOC concentrations, near-surface VOC levels were generally greater than those at higher altitudes, reflecting strong surface source emissions and chemical removal. In Beijing, ethanol exhibited the highest concentration within the PBL with an average of 46.7 ppbv and the largest vertical gradient with a ratio of 16.5 between the below- and above-PBL averages.

The vertical profiles over Beijing and Baoding were compared. Vertical-averaged VOCs above Baoding were generally greater than those in Beijing by factors ranging from 1.2 to 3.5. Increasing trends of concentrations with altitude in Baoding were observed for most VOC species, excluding MVK and MACR, benzene, and toluene. This implies richer precursors available for the secondary pollutant formation above Baoding.

Unlike the general vertical distributions, increases of VOC concentrations above 2500 m altitude were captured in Beijing. According to the ratio analysis, VOC levels near the surface were mainly emitted from vehicular emissions or under the joint impact of vehicular and biomass burning emissions. In contrast, the regional transport of industrial and biomass burning emissions drove the distinct enhancement of VOC concentration above the PBL.

This study presents vertical profiles of key VOC species up to ~4000 m in the core area of the NCP region, yielding valuable insights into VOC distribution patterns within the PBL and in the atmosphere above it. The observed concentration enhancements underscore the substantial impact of regional transport in shaping vertical distributions of VOCs. As these VOCs actively engage in the complex chemical processes above the PBL, the secondary pollutant formation at the higher altitudes necessitates further investigation.

Data availability.

The data in this article are available from the corresponding author upon reasonable request.

Supplement.

The supplement related to this article is available online

Author contributions.

BY and JS designed the research. JS organized the aerial surveys. WZ, FW, PT, WX, YD, and JS contributed to data collection. YH and ZL performed the data analysis, with contributions from BY, SW, and XH. YH, ZL, and BY prepared the article with contributions from SW, XH, and JS. All the authors reviewed the article.

Competing interests.

The authors declare that they have no known competing financial interests that could have appeared to influence the work reported in this paper.

Financial support.

This work was supported by the National Key R&D Program of China (Grant No. 2023YFC3710900, 2023YFC3706103, 2024YFC3013001) and the National Natural Science Foundation of China (Grant No. 42230701, 42121004, 42275188).

Reference

Benish, S. E., He, H., Ren, X., Roberts, S. J., Salawitch, R. J., Li, Z., Wang, F., Wang, Y., Zhang, F., Shao, M., Lu, S., and Dickerson, R. R.: Measurement report: Aircraft observations of ozone, nitrogen oxides, and volatile organic compounds over Hebei Province, China, Atmospheric Chemistry and Physics, 20, 14523-14545, https://doi.org/10.5194/acp-20-14523-2020, 2020.

Canaval, E., Millet, D. B., Zimmer, I., Nosenko, T., Georgii, E., Partoll, E. M., Fischer, L., Alwe, H. D., Kulmala, M., Karl, T., Schnitzler, J. P., and Hansel, A.: Rapid conversion of isoprene photooxidation products in terrestrial plants, Commun Earth Environ, 1, 44, https://doi.org/10.1038/s43247-020-00041-2, 2020.

Cappellin, L., Loreto, F., Biasioli, F., Pastore, P., and McKinney, K.: A mechanism for biogenic production and emission of MEK from MVK decoupled from isoprene biosynthesis, Atmospheric Chemistry and Physics, 19, 3125-3135, https://doi.org/10.5194/acp-19-3125-2019, 2019.

Chang, X., Wang, S., Zhao, B., Xing, J., Liu, X., Wei, L., Song, Y., Wu, W., Cai, S., Zheng, H., Ding, D., and Zheng, M.: Contributions of inter-city and regional transport to PM2.5 concentrations in the Beijing-Tianjin-Hebei region and its implications on regional joint air pollution control, Science of The Total Environment, 660, 1191-1200, https://doi.org/10.1016/j.scitotenv.2018.12.474, 2019.

Chen, S., Wang, H., Lu, K., Zeng, L., Hu, M., and Zhang, Y.: The trend of surface ozone in Beijing from 2013 to 2019: Indications of the persisting strong atmospheric oxidation capacity, Atmospheric Environment, 242, https://doi.org/10.1016/j.atmosenv.2020.117801, 2020.

Coggon, M. M., Veres, P. R., Yuan, B., Koss, A., Warneke, C., Gilman, J. B., Lerner, B. M., Peischl, J., Aikin, K. C., Stockwell, C. E., Hatch, L. E., Ryerson, T. B., Roberts, J. M., Yokelson, R. J., and de Gouw, J. A.: Emissions of nitrogen - containing organic compounds from the burning of herbaceous and arboraceous biomass: Fuel composition dependence and the variability of commonly used nitrile tracers, Geophysical Research Letters, 43, 9903-9912, https://doi.org/10.1002/2016gl070562, 2016.

de Gouw, J., Warneke, C., Holzinger, R., Klüpfel, T., and Williams, J.: Inter-comparison between airborne measurements of methanol, acetonitrile and acetone using two differently configured PTR-MS instruments, International Journal of Mass Spectrometry, 239, 129-137, https://doi.org/10.1016/j.ijms.2004.07.025, 2004.

Dieu Hien, V. T., Lin, C., Thanh, V. C., Kim Oanh, N. T., Thanh, B. X., Weng, C. E., Yuan, C. S., and Rene, E. R.: An overview of the development of vertical sampling technologies for ambient volatile organic compounds (VOCs), Journal of Environmental Management, 247, 401-412, https://doi.org/10.1016/j.jenvman.2019.06.090, 2019.

Fisher, J. A., Jacob, D. J., Travis, K. R., Kim, P. S., Marais, E. A., Chan Miller, C., Yu, K., Zhu, L., Yantosca, R. M., Sulprizio, M. P., Mao, J., Wennberg, P. O., Crounse, J. D., Teng, A. P., Nguyen, T. B., St. Clair, J. M., Cohen, R. C., Romer, P., Nault, B. A., Wooldridge, P. J., Jimenez, J. L., Campuzano-Jost, P., Day, D. A., Hu, W., Shepson, P. B., Xiong, F., Blake, D. R., Goldstein, A. H., Misztal, P. K., Hanisco, T. F., Wolfe, G. M., Ryerson, T. B., Wisthaler, A., and Mikoviny, T.: Organic nitrate chemistry and its implications for nitrogen budgets in an isoprene- and monoterpene-rich atmosphere: constraints from aircraft (SEAC4RS) and ground-based (SOAS) observations in the Southeast US, Atmospheric Chemistry and Physics, 16, 5969-5991, https://doi.org/10.5194/acp-16-5969-2016, 2016.

Forster, E., Bonisch, H., Neumaier, M., Obersteiner, F., Zahn, A., Hilboll, A., Kalisz Hedegaard, A. B., Daskalakis, N., Poulidis, A. P., Vrekoussis, M., Lichtenstern, M., and Braesicke, P.: Chemical and dynamical identification of emission outflows during the HALO campaign EMeRGe in Europe and Asia, Atmospheric Chemistry and Physics, 23, 1893-1918, https://doi.org/10.5194/acp-23-1893-2023, 2023.

Gao, Y., Wang, H., Yuan, L., Jing, S., Yuan, B., Shen, G., Zhu, L., Koss, A., Li, Y., Wang, Q., Huang, D. D., Zhu, S., Tao, S., Lou, S., and Huang, C.: Measurement report: Underestimated reactive organic gases from residential combustion – insights from a near-complete speciation, Atmospheric Chemistry and Physics, 23, 6633-6646, https://doi.org/10.5194/acp-23-6633-2023, 2023.

Han, F., Xu, J., He, Y., Dang, H., Yang, X., and Meng, F.: Vertical structure of foggy haze over the Beijing–Tianjin–Hebei area in January 2013, Atmospheric Environment, 139, 192-204, https://doi.org/10.1016/j.atmosenv.2016.05.030, 2016.

He, X., Yuan, B., Huangfu, Y., Gouw, J. d., Wang, S., Yang, S., Peng, Y., Parrish, D. D., Li, X., Chang, M., Mo, Z., Min, K.-E., Nam, W., Chen, Y., Zhang, X., Qi, J., Xie, Q., Chen, W., Guenther, A., Wang, X., Worsnop, D., Karl, T., and Shao, M.: The critical role of urban greening on managing air quality in cities, Under review, 2025.

564 Holzinger, R., Williams, J., Salisbury, G., Kl¨upfel, T., Reus, M. d., Traub, M., Crutzen, P. J., and
565 Lelieveld, J.: Oxygenated compounds in aged biomass burning plumes over the Eastern Mediterranean:
566 evidence for strong secondary production ofmethanol and acetone, Atmospheric Chemistry and Physics,
567 5, https://doi.org/10.5194/acp-5-39-2005, 2005.
568 Hu, D., Li, X., Chen, Z., Cui, Y., Gu, F., Jia, F., Xiao, T., Su, H., Xu, J., Wang, H., Wu, P., and Zhang, Y.:
569 Performance and extracellular polymers substance analysis of a pilot scale anaerobic membrane
570 bioreactor for treating tetrahydrofuran pharmaceutical wastewater at different HRTs, Journal of
571 Hazardous Materials, 342, 383-391, 10.1016/j.jhazmat.2017.08.028, 2018.
572 Huang, Z., Hong, L., Yin, P., Wang, X., and Zhang, Y.: Source Apportionment and Transport
573 Characteristics of Ozone in Baoding during Summer Time, Acta Scientiarum Naturalium Universitatis
574 Pekinensis, 53, 665-672, 10.13209/j.0479-8023.2017.189, 2018.
575 Huangfu, Y., Yuan, B., Wang, S., Wu, C., He, X., Qi, J., de Gouw, J., Warneke, C., Gilman, J. B., Wisthaler,
576 A., Karl, T., Graus, M., Jobson, B. T., and Shao, M.: Revisiting Acetonitrile as Tracer of Biomass Burning
577 in Anthropogenic - Influenced Environments, Geophysical Research Letters, 48,
578 https://doi.org/10.1029/2020gl092322, 2021.
579 Inomata, S., Tanimoto, H., Fujitani, Y., Sekimoto, K., Sato, K., Fushimi, A., Yamada, H., Hori, S.,
580 Kumazawa, Y., Shimono, A., and Hikida, T.: On-line measurements of gaseous nitro-organic compounds
581 in diesel vehicle exhaust by proton-transfer-reaction mass spectrometry, Atmospheric Environment, 73,
582 195-203, https://doi.org/10.1016/j.atmosenv.2013.03.035, 2013.
583 Jiang, C., Pei, C., Cheng, C., Shen, H., Zhang, Q., Lian, X., Xiong, X., Gao, W., Liu, M., Wang, Z.,
584 Huang, B., Tang, M., Yang, F., Zhou, Z., and Li, M.: Emission factors and source profiles of volatile
585 organic compounds from typical industrial sources in Guangzhou, China, Science of the Total
586 Environment, 869, 161758, https://doi.org/10.1016/j.scitotenv.2023.161758, 2023.
587 Karion, A., Sweeney, C., Kort, E. A., Shepson, P. B., Brewer, A., Cambaliza, M., Conley, S. A., Davis,
588 K., Deng, A., Hardesty, M., Herndon, S. C., Lauvaux, T., Lavoie, T., Lyon, D., Newberger, T., Petron, G.,
589 Rella, C., Smith, M., Wolter, S., Yacovitch, T. I., and Tans, P.: Aircraft-Based Estimate of Total Methane
590 Emissions from the Barnett Shale Region, Environmental Science & Technology, 49, 8124-8131,
591 https://doi.org/10.1021/acs.est.5b00217, 2015.

592 Kwak, K.-H., Lee, S.-H., Kim, A. Y., Park, K.-C., Lee, S.-E., Han, B.-S., Lee, J., and Park, Y.-S.: Daytime
593 Evolution of Lower Atmospheric Boundary Layer Structure: Comparative Observations between a 307-
594 m Meteorological Tower and a Rotary-Wing UAV, Atmosphere, 11,
595 https://doi.org/10.3390/atmos11111142, 2020.
596 Le, T., Wang, Y., Liu, L., Yang, J., Yung, Y. L., Li, G., and Seinfeld, J. H.: Unexpected air pollution with
597 marked emission reductions during the COVID-19 outbreak in China, Science, 369, 702-706,
598 https://doi.org/10.1126/science.abb7431, 2020.
599 Li, K., Jacob, D. J., Liao, H., Shen, L., Zhang, Q., and Bates, K. H.: Anthropogenic drivers of 2013-2017
600 trends in summer surface ozone in China, Proceedings of the National Academy of Sciences of the United
601 States of America, 116, 422-427, https://doi.org/10.1073/pnas.1812168116, 2019a.
602 Li, M., Zhang, Q., Zheng, B., Tong, D., Lei, Y., Liu, F., Hong, C., Kang, S., Yan, L., Zhang, Y., Bo, Y.,
603 Su, H., Cheng, Y., and He, K.: Persistent growth of anthropogenic non-methane volatile organic
604 compound (NMVOC) emissions in China during 1990–2017: drivers, speciation and ozone formation
605 potential, Atmospheric Chemistry and Physics, 19, 8897-8913, https://doi.org/10.5194/acp-19-8897-
606 2019, 2019b.
607 Li, X.-B., Yuan, B., Huangfu, Y., Yang, S., Song, X., Qi, J., He, X., Wang, S., Chen, Y., Yang, Q., Song,
608 Y., Peng, Y., Tang, G., Gao, J., and Shao, M.: Vertical changes in volatile organic compounds (VOCs)
609 and impacts on photochemical ozone formation, Atmospheric Chemistry and Physics, 25, 2459–2472,
610 https://doi.org/10.5194/acp-25-2459-2025, 2024.
611 Li, X. B., Yuan, B., Wang, S., Wang, C., Lan, J., Liu, Z., Song, Y., He, X., Huangfu, Y., Pei, C., Cheng,
612 P., Yang, S., Qi, J., Wu, C., Huang, S., You, Y., Chang, M., Zheng, H., Yang, W., Wang, X., and Shao, M.:
613 Variations and sources of volatile organic compounds (VOCs) in urban region: insights from
614 measurements on a tall tower, Atmospheric Chemistry and Physics, 22, 10567-10587,
615 https://doi.org/10.5194/acp-22-10567-2022, 2022a.
616 Li, Z., Yu, S., Li, M., Chen, X., Zhang, Y., Song, Z., Li, J., Jiang, Y., Liu, W., Li, P., and Zhang, X.: The
617 Modeling Study about Impacts of Emission Control Policies for Chinese 14th Five-Year Plan on PM2.5
618 and O3 in Yangtze River Delta, China, Atmosphere, 13, 26, https://doi.org/10.3390/atmos13010026,
619 2022b.

Liu, K., Quan, J., Mu, Y., Zhang, Q., Liu, J., Gao, Y., Chen, P., Zhao, D., and Tian, H.: Aircraft measurements of BTEX compounds around Beijing city, Atmospheric Environment, 73, 11-15, https://doi.org/10.1016/j.atmosenv.2013.02.050, 2013.

Liu, Q., Ding, D., Huang, M., Tian, P., Zhao, D., Wang, F., Li, X., Bi, K., Sheng, J., Zhou, W., Liu, D., Huang, R., and Zhao, C.: A study of elevated pollution layer over the North China Plain using aircraft measurements, Atmospheric Environment, 190, 188-194, https://doi.org/10.1016/j.atmosenv.2018.07.024, 2018.

Liu, Y., Wang, H., Jing, S., Gao, Y., Peng, Y., Lou, S., Cheng, T., Tao, S., Li, L., Li, Y., Huang, D., Wang, Q., and An, J.: Characteristics and sources of volatile organic compounds (VOCs) in Shanghai during summer: Implications of regional transport, Atmospheric Environment, 215, https://doi.org/10.1016/j.atmosenv.2019.116902, 2019.

Lu, X., Zhang, L., Chen, Y., Zhou, M., Zheng, B., Li, K., Liu, Y., Lin, J., Fu, T.-M., and Zhang, Q.: Exploring 2016–2017 surface ozone pollution over China: source contributions and meteorological influences, Atmospheric Chemistry and Physics, 19, 8339-8361, https://doi.org/10.5194/acp-19-8339-2019, 2019.

Lu, X., Zhang, L., Wang, X., Gao, M., Li, K., Zhang, Y., Yue, X., and Zhang, Y.: Rapid Increases in Warm-Season Surface Ozone and Resulting Health Impact in China Since 2013, Environmental Science & Technology Letters, 7, 240-247, https://doi.org/10.1021/acs.estlett.0c00171, 2020.

Mao, Z., Bai, Y., and Meng, F.: How can China achieve the energy and environmental targets in the 14th and 15th five-year periods? A perspective of economic restructuring, Sustainable Production and Consumption, 27, 2022-2036, https://doi.org/10.1016/j.spc.2021.05.005, 2021.

Peng, Z.-R., Wang, D., Wang, Z., Gao, Y., and Lu, S.: A study of vertical distribution patterns of PM2.5 concentrations based on ambient monitoring with unmanned aerial vehicles: A case in Hangzhou, China, Atmospheric Environment, 123, 357-369, https://doi.org/10.1016/j.atmosenv.2015.10.074, 2015.

Ren, X., Salmon, O. E., Hansford, J. R., Ahn, D., Hall, D., Benish, S. E., Stratton, P. R., He, H., Sahu, S., Grimes, C., Heimburger, A. M. F., Martin, C. R., Cohen, M. D., Stunder, B., Salawitch, R. J., Ehrman, S. H., Shepson, P. B., and Dickerson, R. R.: Methane Emissions From the Baltimore-Washington Area

Based on Airborne Observations: Comparison to Emissions Inventories, Journal of Geophysical Research: Atmospheres, 123, 8869-8882, https://doi.org/10.1029/2018jd028851, 2018.

Sangiorgi, G., Ferrero, L., Perrone, M. G., Bolzacchini, E., Duane, M., and Larsen, B. R.: Vertical distribution of hydrocarbons in the low troposphere below and above the mixing height: Tethered balloon measurements in Milan, Italy, Environmental Pollution, 159, 3545-3552, https://doi.org/10.1016/j.envpol.2011.08.012, 2011.

Shi, H., Critto, A., Torresan, S., and Gao, Q.: The Temporal and Spatial Distribution Characteristics of Air Pollution Index and Meteorological Elements in Beijing, Tianjin, and Shijiazhuang, China, Integrated Environmental Assessment and Management, 14, 710-721, https://doi.org/10.1002/ieam.4067, 2018.

Squires, F. A., Nemitz, E., Langford, B., Wild, O., Drysdale, W. S., Acton, W. J. F., Fu, P., Grimmond, C. S. B., Hamilton, J. F., Hewitt, C. N., Hollaway, M., Kotthaus, S., Lee, J., Metzger, S., Pingintha-Durden, N., Shaw, M., Vaughan, A. R., Wang, X., Wu, R., Zhang, Q., and Zhang, Y.: Measurements of traffic-dominated pollutant emissions in a Chinese megacity, Atmospheric Chemistry and Physics, 20, 8737-8761, https://doi.org/10.5194/acp-20-8737-2020, 2020.

Sun, J., Wang, Y., Wu, F., Tang, G., Wang, L., Wang, Y., and Yang, Y.: Vertical characteristics of VOCs in the lower troposphere over the North China Plain during pollution periods, Environmental Pollution, 236, 907-915, https://doi.org/10.1016/j.envpol.2017.10.051, 2018.

Valach, A. C., Langford, B., Nemitz, E., MacKenzie, A. R., and Hewitt, C. N.: Concentrations of selected volatile organic compounds at kerbside and background sites in central London, Atmospheric Environment, 95, 456-467, https://doi.org/10.1016/j.atmosenv.2014.06.052, 2014.

Vo, T. D., Lin, C., Weng, C. E., Yuan, C. S., Lee, C. W., Hung, C. H., Bui, X. T., Lo, K. C., and Lin, J. X.: Vertical stratification of volatile organic compounds and their photochemical product formation potential in an industrial urban area, Journal of Environmental Management, 217, 327-336, https://doi.org/10.1016/j.jenvman.2018.03.101, 2018.

Vogelezang, D. H. P., and Holtslag, A. A. M.: Evaluation and model impacts of alternative boundary-layer height formulations, Boundary-Layer Meteorology, 81, 245-269, https://doi.org/10.1007/BF02430331, 1996.

Wang, M., Shao, M., Chen, W., Yuan, B., Lu, S., Zhang, Q., Zeng, L., and Wang, Q.: A temporally and spatially resolved validation of emission inventories by measurements of ambient volatile organic compounds in Beijing, China, Atmospheric Chemistry and Physics, 14, 5871-5891, https://doi.org/10.5194/acp-14-5871-2014, 2014.

Wang, M., Shao, M., Chen, W., Lu, S., Liu, Y., Yuan, B., Zhang, Q., Zhang, Q., Chang, C. C., Wang, B., Zeng, L., Hu, M., Yang, Y., and Li, Y.: Trends of non-methane hydrocarbons (NMHC) emissions in Beijing during 2002–2013, Atmospheric Chemistry and Physics, 15, 1489-1502, 10.5194/acp-15-1489-2015, 2015.

Wang, Q., Shao, M., Liu, Y., William, K., Paul, G., Li, X., Liu, Y., and Lu, S.: Impact of biomass burning on urban air quality estimated by organic tracers: Guangzhou and Beijing as cases, Atmospheric Environment, 41, 8380-8390, https://doi.org/10.1016/j.atmosenv.2007.06.048, 2007.

Wang, S., Yuan, B., Wu, C., Wang, C., Li, T., He, X., Huangfu, Y., Qi, J., Li, X.-B., Sha, Q. e., Zhu, M., Lou, S., Wang, H., Karl, T., Graus, M., Yuan, Z., and Shao, M.: Oxygenated volatile organic compounds (VOCs) as significant but varied contributors to VOC emissions from vehicles, Atmospheric Chemistry and Physics, 22, 9703-9720, https://doi.org/10.5194/acp-22-9703-2022, 2022.

Wang, S., Yuan, B., He, X., Cui, R., Song, X., Chen, Y., Wu, C., Wang, C., Huangfu, Y., Li, X.-B., Wang, B., and Shao, M.: Emission characteristics of reactive organic gases (ROGs) from industrial volatile chemical products (VCPs) in the Pearl River Delta (PRD), China, Atmospheric Chemistry and Physics, 24, 7101-7121, https://doi.org/10.5194/acp-24-7101-2024, 2024.

Wang, Z., Zhang, P., Pan, L., Qian, Y., Li, Z., Li, X., Guo, C., Zhu, X., Xie, Y., and Wei, Y.: Ambient Volatile Organic Compound Characterization, Source Apportionment, and Risk Assessment in Three Megacities of China in 2019, Toxics, 11, https://doi.org/10.3390/toxics11080651, 2023.

Wilde, S. E., Dominutti, P. A., Allen, G., Andrews, S. J., Bateson, P., Bauguitte, S. J. B., Burton, R. R., Colfescu, I., France, J., Hopkins, J. R., Huang, L., Jones, A. E., Lachlan-Cope, T., Lee, J. D., Lewis, A. C., Mobbs, S. D., Weiss, A., Young, S., and Purvis, R. M.: Speciation of VOC emissions related to offshore North Sea oil and gas production, Atmospheric Chemistry and Physics, 21, 3741-3762, https://doi.org/10.5194/acp-21-3741-2021, 2021.

Wu, C., Wang, C., Wang, S., Wang, W., Yuan, B., Qi, J., Wang, B., Wang, H., Wang, C., Song, W., Wang, X., Hu, W., Lou, S., Ye, C., Peng, Y., Wang, Z., Huangfu, Y., Xie, Y., Zhu, M., Zheng, J., Wang, X., Jiang, B., Zhang, Z., and Shao, M.: Measurement report: Important contributions of oxygenated compounds to emissions and chemistry of volatile organic compounds in urban air, Atmospheric Chemistry and Physics, 20, 14769-14785, https://doi.org/10.5194/acp-20-14769-2020, 2020a.

Wu, J., Gao, S., Chen, X., Yang, Y., Fu, Q.-Y., Che, X., and Jiao, Z.: Source Profiles and Impact of Volatile Organic Compounds in the Coating Manufacturing Industry, Environmental Science, 41, 1582-1588, https://doi.org/10.13227/j.hjkx.201908203, 2020b.

Wu, R., Li, J., Hao, Y., Li, Y., Zeng, L., and Xie, S.: Evolution process and sources of ambient volatile organic compounds during a severe haze event in Beijing, China, Science of The Total Environment, 560-561, 62-72, https://doi.org/10.1016/j.scitotenv.2016.04.030, 2016.

Xue, L. K., Wang, T., Simpson, I. J., Ding, A. J., Gao, J., Blake, D. R., Wang, X. Z., Wang, W. X., Lei, H. C., and Jing, D. Z.: Vertical distributions of non-methane hydrocarbons and halocarbons in the lower troposphere over northeast China, Atmospheric Environment, 45, 6501-6509, 10.1016/j.atmosenv.2011.08.072, 2011.

Yang, Q., Li, X.-B., Yuan, B., Zhang, X., Huangfu, Y., Yang, L., He, X., Qi, J., and Shao, M.: Measurement report: Enhanced photochemical formation of formic and isocyanic acids in urban regions aloft – insights from tower-based online gradient measurements, Atmospheric Chemistry and Physics, 24, 6865-6882, https://doi.org/10.5194/acp-24-6865-2024, 2024a.

Yang, S., Zhu, B., Shi, S., Jiang, Z., Hou, X., An, J., and Xia, L.: Vertical Features of Volatile Organic Compounds and Their Potential Photochemical Reactivities in Boundary Layer Revealed by In-Situ Observations and Satellite Retrieval, Remote Sensing, 16, 10.3390/rs16081403, 2024b.

Yao, D., Tang, G., Sun, J., Wang, Y., Yang, Y., Wang, Y., Liu, B., He, H., and Wang, Y.: Annual nonmethane hydrocarbon trends in Beijing from 2000 to 2019, Journal of Environmental Sciences, 112, 210-217, 10.1016/j.jes.2021.04.017, 2022a.

Yao, D., Tang, G., Wang, Y., Yang, Y., Wang, Y., Liu, Y., Yu, M., Liu, Y., Yu, H., Liu, J., Hu, B., Wang, P., and Wang, Y.: Oscillation cumulative volatile organic compounds on the northern edge of the North

China Plain: Impact of mountain-plain breeze, Science of The Total Environment, 821, 153541, https://doi.org/10.1016/j.scitotenv.2022.153541, 2022b.

Yuan, B., Shao, M., de Gouw, J., Parrish, D. D., Lu, S., Wang, M., Zeng, L., Zhang, Q., Song, Y., Zhang, J., and Hu, M.: Volatile organic compounds (VOCs) in urban air: How chemistry affects the interpretation of positive matrix factorization (PMF) analysis, Journal of Geophysical Research: Atmospheres, 117, n/a-n/a, https://doi.org/10.1029/2012jd018236, 2012.

Yuan, B., Koss, A. R., Warneke, C., Coggon, M., Sekimoto, K., and de Gouw, J. A.: Proton-Transfer-Reaction Mass Spectrometry: Applications in Atmospheric Sciences, Chemical Reviews, 117, 13187-13229, https://doi.org/10.1021/acs.chemrev.7b00325, 2017.

Zhang, H., Zhang, Y., Huang, Z., Acton, W. J. F., Wang, Z., Nemitz, E., Langford, B., Mullinger, N., Davison, B., Shi, Z., Liu, D., Song, W., Yang, W., Zeng, J., Wu, Z., Fu, P., Zhang, Q., and Wang, X.: Vertical profiles of biogenic volatile organic compounds as observed online at a tower in Beijing, Journal of Environmental Sciences, 95, 33-42, https://doi.org/10.1016/j.jes.2020.03.032, 2020.

Zhang, K., Xiu, G., Zhou, L., Bian, Q., Duan, Y., Fei, D., Wang, D., and Fu, Q.: Vertical distribution of volatile organic compounds within the lower troposphere in late spring of Shanghai, Atmospheric Environment, 186, 150-157, https://doi.org/10.1016/j.atmosenv.2018.03.044, 2018.

Zhang, K., Zhou, L., Fu, Q., Yan, L., Bian, Q., Wang, D., and Xiu, G.: Vertical distribution of ozone over Shanghai during late spring: A balloon-borne observation, Atmospheric Environment, 208, 48-60, https://doi.org/10.1016/j.atmosenv.2019.03.011, 2019.

Zhang, Y., Gao, Z., Li, D., Li, Y., Zhang, N., Zhao, X., and Chen, J.: On the computation of planetary boundary-layer height using the bulk Richardson number method, Geoscientific Model Development, 7, 2599-2611, https://doi.org/10.5194/gmd-7-2599-2014, 2014.

Zhao, D., Huang, M., Tian, P., He, H., Lowe, D., Zhou, W., Sheng, J., Wang, F., Bi, K., Kong, S., Yang, Y., Liu, Q., Liu, D., and Ding, D.: Vertical characteristics of black carbon physical properties over Beijing region in warm and cold seasons, Atmospheric Environment, 213, 296-310, https://doi.org/10.1016/j.atmosenv.2019.06.007, 2019.

Zhao, D., Liu, D., Yu, C., Tian, P., Hu, D., Zhou, W., Ding, S., Hu, K., Sun, Z., Huang, M., Huang, Y., Yang, Y., Wang, F., Sheng, J., Liu, Q., Kong, S., Li, X., He, H., and Ding, D.: Vertical evolution of black

carbon characteristics and heating rate during a haze event in Beijing winter, Science of The Total Environment, 709, https://doi.org/10.1016/j.scitotenv.2019.136251, 2020.

Zhao, R., Yin, B., Zhang, N., Wang, J., Geng, C., Wang, X., Han, B., Li, K., Li, P., Yu, H., Yang, W., and Bai, Z.: Aircraft-based observation of gaseous pollutants in the lower troposphere over the Beijing-Tianjin-Hebei region, Science of The Total Environment, 773, https://doi.org/10.1016/j.scitotenv.2020.144818, 2021.

Zhong, Z., Sha, Q., Zheng, J., Yuan, Z., Gao, Z., Ou, J., Zheng, Z., Li, C., and Huang, Z.: Sector-based VOCs emission factors and source profiles for the surface coating industry in the Pearl River Delta region of China, Science of the Total Environment, 583, 19-28, https://doi.org/10.1016/j.scitotenv.2016.12.172, 2017.

Zhu, B., Yang, S., Shi, S., Jiang, Z., Tang, G., Lu, C., Hou, X., An, J., Xia, L., and Liao, H.: Revealing Distinct Photochemical Ages within the Vertical Boundary Layer and Seasons by Observed VOC Species Ratios, ACS ES&T Air, 2, 1172-1179, 10.1021/acsestair.4c00319, 2025.

Table 1. Detailed information for different flight routes during different aerial surveys in Sep. 2017 and Jul. 2019.

Route number	Main area	Main altitude (m)	Date	Profile time*	
				Ascending stage	Descending stage
Route 1	Beijing	~3800	Sep. 09, 2017	12:06-12:29	12:31-16:54
Route 2	Beijing	~3800	Sep. 12, 2017	12:16-12:46	12:55-16:10
Route 3	Beijing	~3800	Sep. 13, 2017	13:35-14:11	14:30-16:55
Route 4	Beijing	~3700	Sep. 15, 2017	10:36-11:00	11:00-13:05
Route 5	Beijing	~2500/~2800	Sep. 14, 2017	12:31-12:46	16:00-16:58
	Baoding	2200-3500	Sep. 14, 2017	-	-
Route 6	Beijing	~3100	Jul. 14, 2019	9:41-10:14	11:43-12:18
	Baoding	~3090	Jul. 14, 2019	11:21-11:28	10:18-11:17

Note: * Profile time is the local time.

Formatted Table

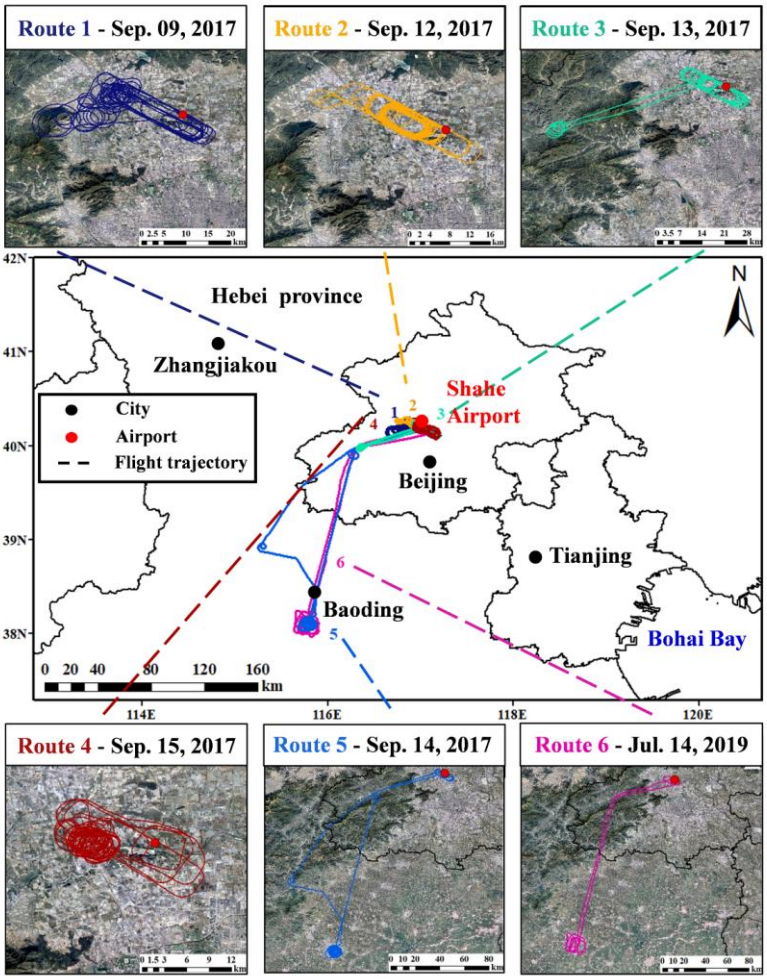

Figure 1. Flight trajectories during different aerial surveys in Sep. 2017 and Jul. 2019. Figures were made by Meteolnfo software. The satellite images were downloaded from Google Earth and edited in ArcGIS 10.8.

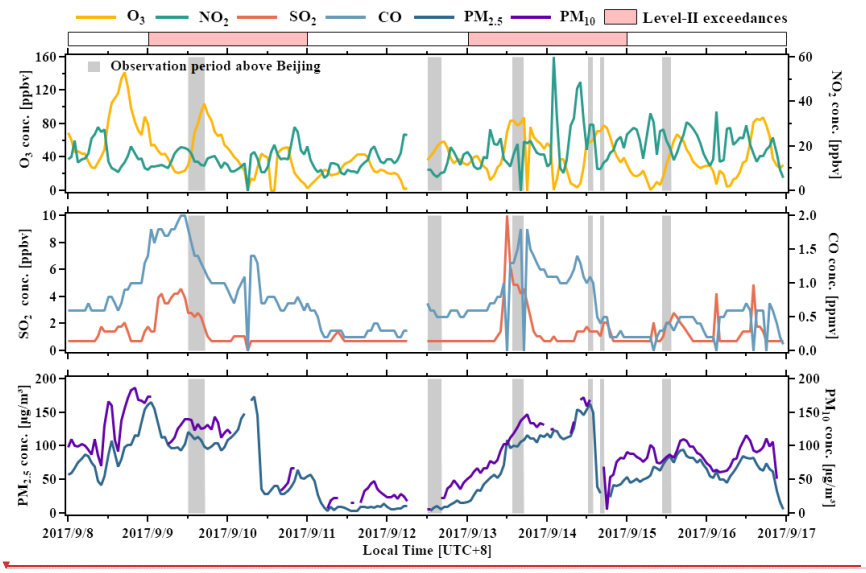

Figure 2. Time series of criteria pollutants including ozone, NO_2, SO_2, CO, $PM_{2.5}$, and PM_{10} from Sep. 8th to 16th, 2017. Data is obtained from Changping Town stations, the closest national air quality monitoring stations to the airport. Grey shaded areas indicate the observation periods. The bars filled with light red at the bottom show the periods when Level-II National Ambient Air Quality Standards (NAAQS) were exceeded.

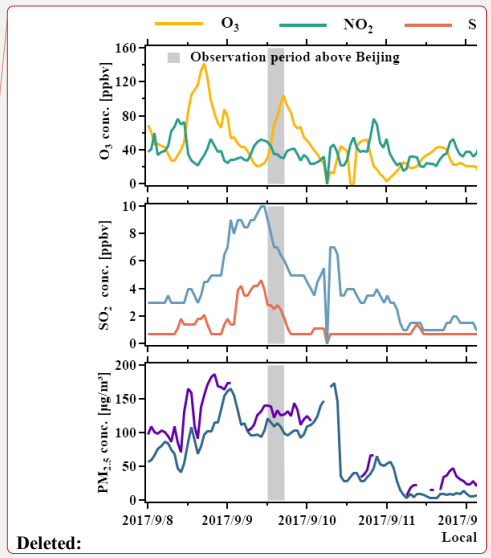

Deleted:

Deleted: S

Deleted:

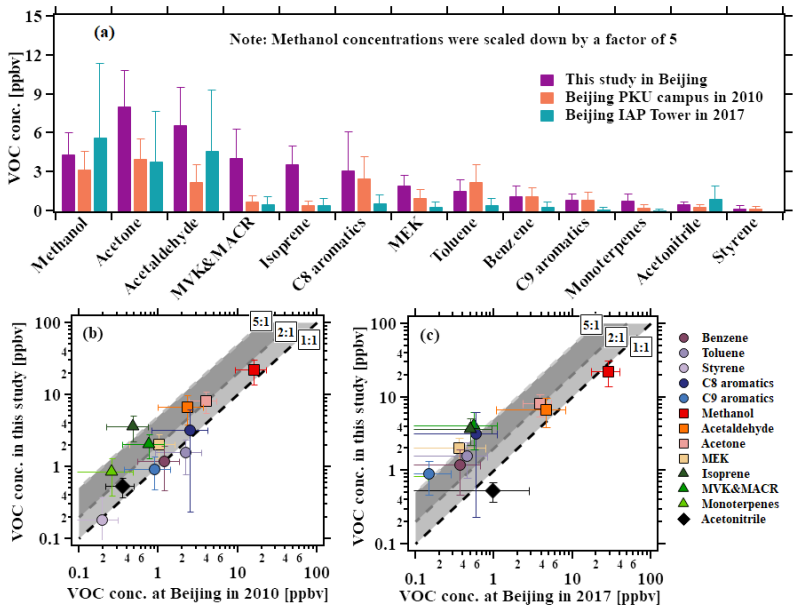

789

790 **Figure 3**. Comparison of averaged VOC concentrations below the PBL in this study
791 and those measured in Beijing in 2010 (Yuan et al., 2012) and 2017 (Squires et al.,
792 2020). Methanol concentrations were scaled down by a factor of 5 to improve
793 visualization in (a). Scatter plots were also shown in (b) and (c). Error bars indicate the
794 standard deviations. Reference lines are shown with shading to illustrate the differences.

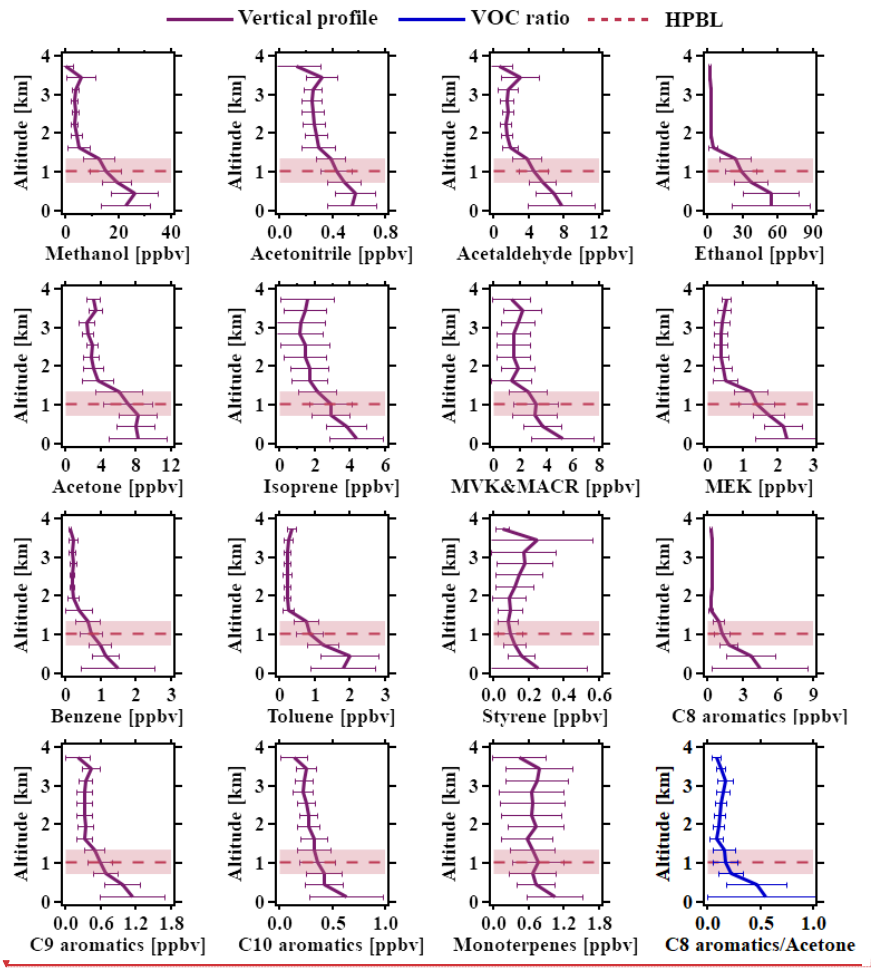

Deleted:

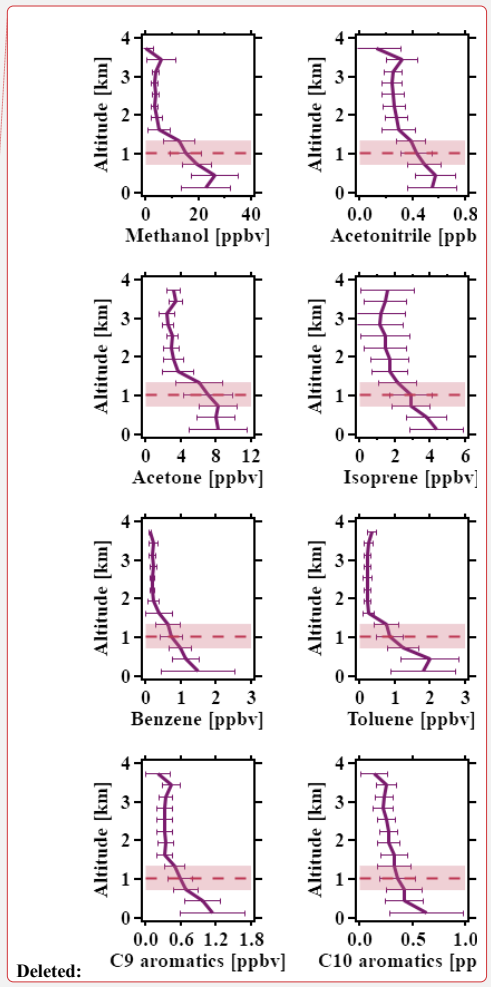

Figure 4. Averaged vertical profile (purple line) of VOCs in five aerial surveys above the Beijing area in Sep. 2017 with error bar. The blue line shows the average vertical profile of C8 aromatics-to-acetone concentration ratio with error bar. The red dashed line is the average of the HPBL, with the light red area showing the variation range of one standard deviation.

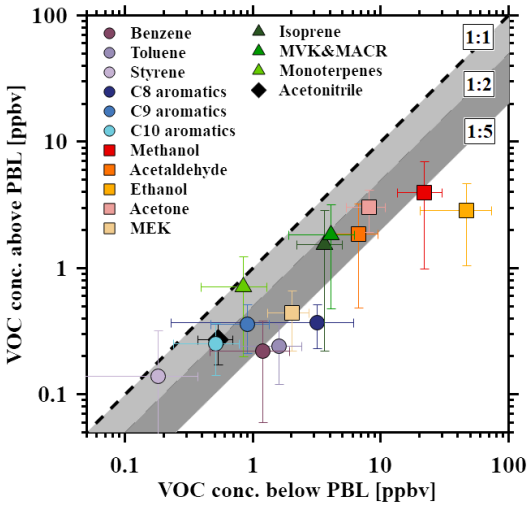

803

804 **Figure 5.** Scatter plot of the averaged VOC concentrations in Beijing below and above
805 the PBL in Sep. 2017. Error bars indicate the standard deviations. Reference lines are
806 shown with shading to illustrate the differences.

807

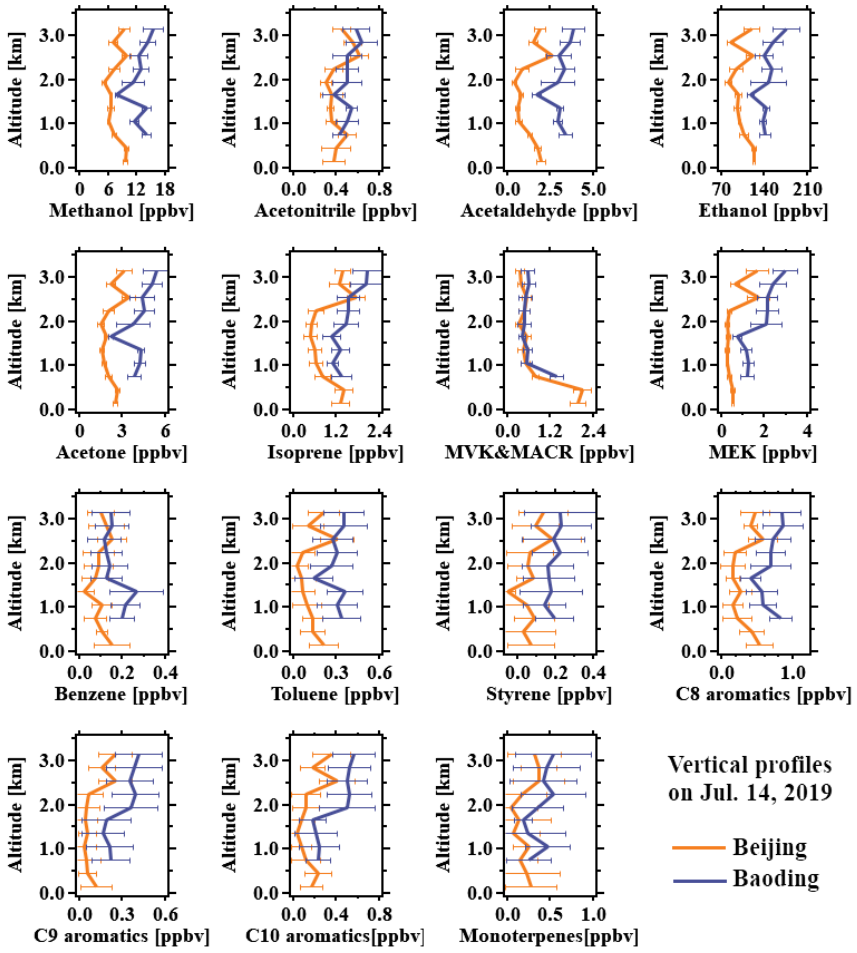

808

809 **Figure 6.** Comparison of vertical profiles of VOCs in Beijing (in orange) and Baoding

810 (in blue) during the aerial survey on Jul. 14th, 2019, with error bars. The data measured

811 during the descending stages above both cities were plotted.

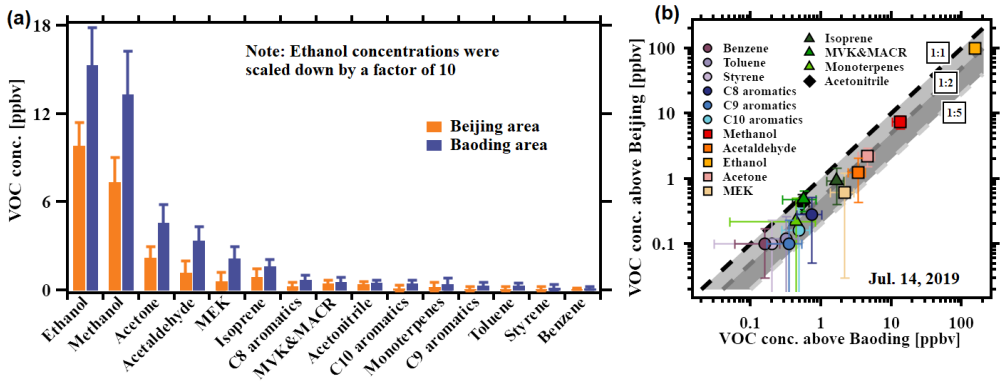

812

813 **Figure 7.** Comparison of averaged VOC vertical concentrations in Beijing and Baoding during the aerial survey on Jul. 14th, 2019. The data
814 measured within the same altitude range (500 m - 3000 m) were averaged. Ethanol concentrations were scaled down by a factor of 10 to improve
815 visualization in (a). The scatter plot was made in (b). Error bars indicate the standard deviations. Reference lines are shown with shading to
816 illustrate the differences.

817

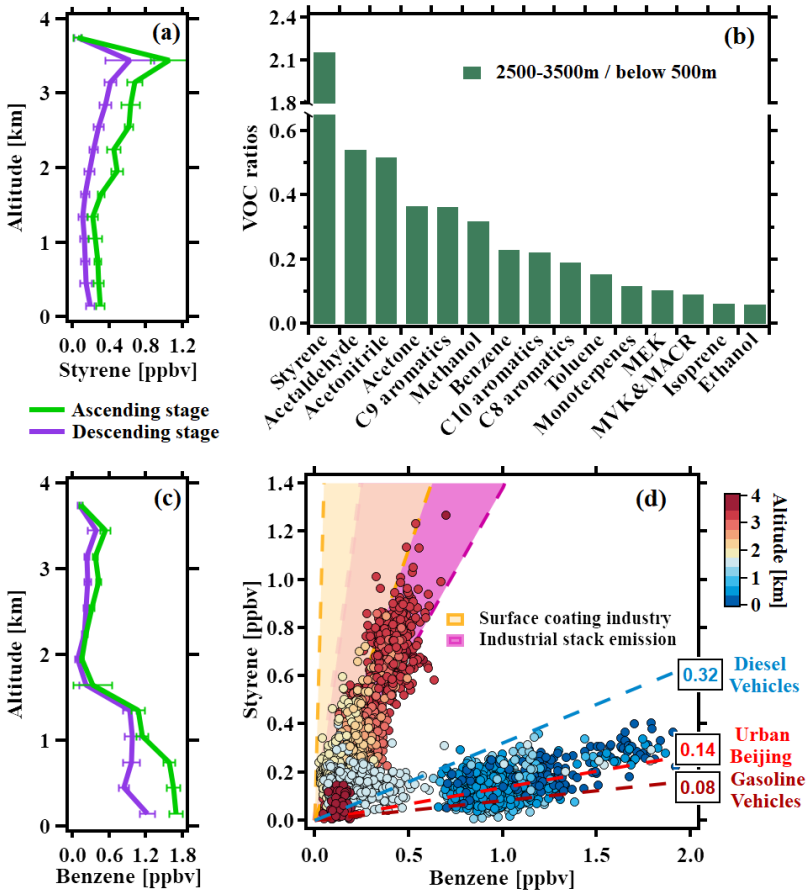

Figure 8. Analysis of the vertical profiles of styrene (a) and benzene (c) during ascending (in green) and descending (in purple) stages with error bars on Sep. 9th, 2017. (b) The ratios of each VOC species measured between 2500-3500 m and below 500 m. (d) The correlation analysis between styrene and benzene using the profiles. All the data points were color-coded with altitudes. Areas shaded with orange and purple represent the typical ratio ranges of styrene and benzene for the surface coating industry (Zhong et al., 2017) and industrial stack emissions (Jiang et al., 2023), respectively, showing an overlap between the two. The blue and dark red dashed lines represent ratios of styrene and benzene for diesel and gasoline vehicular emissions, respectively (Wang et al., 2024). The red dashed line represents the ratio measured in urban Beijing at the IAP tower in 2021 (He et al., 2025).

Deleted: The area with orange shadows represents the

Deleted: in

Deleted: . The area with purple shadows represents the ratio ranges in typical

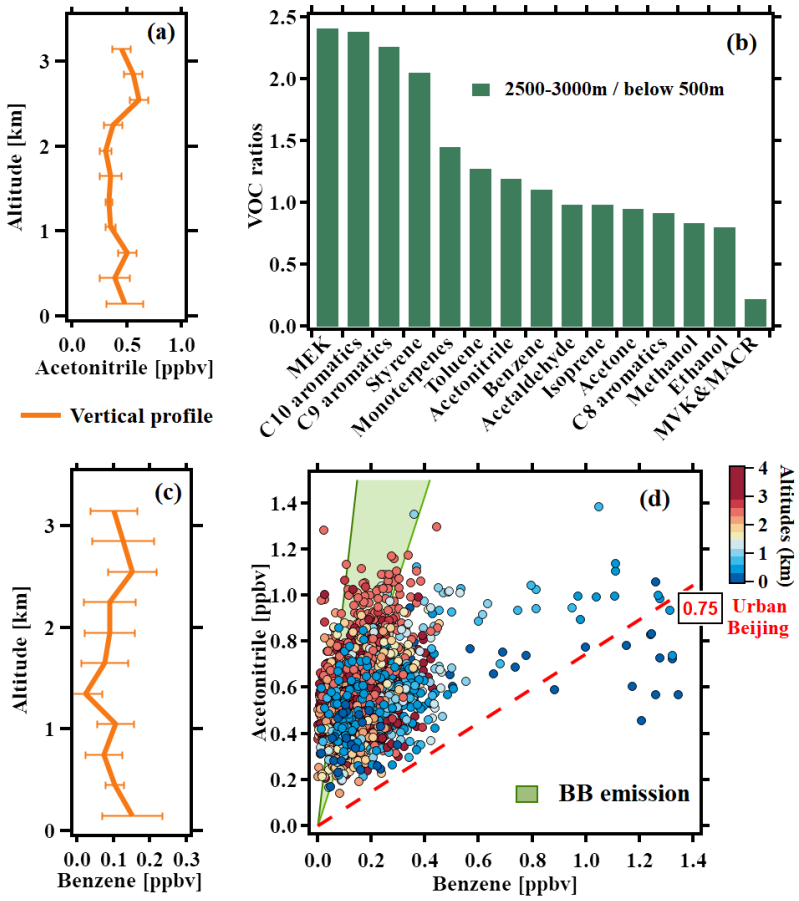

834

835 **Figure 9.** Analysis of the vertical profiles of acetonitrile (a) and benzene (c) with error
836 bars on Jul. 14th, 2019. (b) The ratios of each VOC species measured between 2500-
837 3000 m and below 500 m. (d) The correlation analysis between acetonitrile and benzene
838 using the whole flight data. All the data points were color-coded with altitudes. The red
839 dashed lines represent ratios in urban Beijing at the IAP tower in 2021 (He et al., 2025).
840 The area with green shadow represents the ratio ranges of acetonitrile and benzene
841 measured in the biomass burning (BB) emissions, including wood, corncob, corn straw,
842 and bean straw (Gao et al., 2023).

Deleted:

Deleted: profiles